

Neutron spin echo measurements of the diffusion of water in porous solids

This article has been downloaded from IOPscience. Please scroll down to see the full text article.

1993 J. Phys.: Condens. Matter 5 7529

(<http://iopscience.iop.org/0953-8984/5/41/001>)

View [the table of contents for this issue](#), or go to the [journal homepage](#) for more

Download details:

IP Address: 171.66.16.96

The article was downloaded on 11/05/2010 at 01:59

Please note that [terms and conditions apply](#).

Neutron spin echo measurements of the diffusion of water in porous solids

J-C Li†‡, D K Ross‡ and C Lartigue§

† Department of Physics, University of Birmingham, Birmingham B15 2TT, UK

‡ Department of Pure and Applied Physics, University of Salford, Salford M6 5WT, UK

§ Institut Laue–Langevin, 156X Centre de Tri, 38042 Grenoble, France

Received 1 February 1993, in final form 15 July 1993

Abstract. The tracer diffusion of a liquid in a porous media was studied using the neutron spin echo technique. The samples used consisted of porous Vycor glass saturated with a mixture of D₂O/H₂O (64/36) water to match out the coherent small-angle scattering component due to the neutron scattering density contrast between water and the Vycor matrix, in order to reduce the small-angle neutron scattering and the chemical diffusion contribution to the quasi-elastic scattering. A series of measurements has been made in the Q range 0.07–0.14 Å⁻¹ using the spin echo spectrometer IN11 at the ILL. This experiment in principle enables us to measure the tracer diffusion coefficient of the liquid within a pore and through the local pore network and hence to investigate the interconnectivity of these pores through a determination of $\langle r^2(t) \rangle$ over length scales to about 100 Å.

1. Introduction

Porous Vycor silica glass has, in the past, been extensively studied as a model for a porous rock using a number of techniques both in relation to its structure [1–3] and to various other properties [4–8]. The physicist's interest stems from the question of how to describe the geometry of individual pores, how they are arranged relative to the neighbouring pores and how to describe systematically the interconnection between adjacent pores, and from a general interest in the properties of liquids in small pores. Quasi-elastic neutron scattering (QENS) is a unique technique in that it provides otherwise unobtainable information about liquid flow through porous media. This is currently a topic of considerable fundamental interest and also has practical significance, in particular due to the need to understand low rates of liquid flow under pressure gradients in the oil industry. When the measurements are extended towards low Q by means of the spin echo technique, one can measure diffusion over a local network of pores and hence can investigate their interconnectivity through a determination of $\langle r^2(t) \rangle$ in the appropriate length range. This essentially provides us with a new approach to the geometric description of the distribution of pore sizes and interconnections, both in terms of traditional theories involving tortuosity factors and of more recent speculations about the relationship between the fractal description of a system and the way in which $\langle r^2(t) \rangle$ varies with time over the range of r values where a fractal description is appropriate [9–11]. As oil shales [12] and other rocks [13] have been shown to exhibit fractal behaviour, i.e. the scattering intensity varies as Q^{-n} with $3 < n < 4$ for different shales, these interesting ideas may have considerable practical importance.

For many years, light scattering has been used to study the dynamics and structures of colloidal suspensions, where both the particle size and the spatial correlation lengths are of

the order of the wavelength of light (4000–7000 Å). Tracer diffusion coefficients measured by this technique are obviously measured over distances that are very large compared to the fractal range in porous solids. Light scattering techniques have also been used to measure the tracer diffusion coefficient of optically active molecules in porous solids [9]. Here, one is also interested in the chemical diffusion coefficient of the liquid as this can be related to the flow rate of the liquid through the solid under the influence of a chemical potential via the compressibility. For a fractal system with a lower characteristic dimension of approximately the pore dimension (20–30 Å) and an upper limit of some hundreds of ångströms, small-angle x-ray and neutron scattering are the appropriate techniques to use. Neutron scattering is particularly useful because of the contrast variation technique and the possibility of using quasi-elastic scattering. The spin echo spectrometer IN11 at the ILL, Grenoble is specifically designed for this type of experiment with very high resolution in energy transfer (10^{-7} eV) at small angles of scatter (low Q). The principle of this technique is similar to the NMR technique of the same name. The very high-energy resolution is achieved by making two time measurements on the same neutron as opposed to the more usual time-of-flight technique of defining the time origin by pulsing the beam. In the latter technique, the use of a short enough pulse and a long enough flight path to achieve the above resolution would involve sacrificing so much intensity as to make the measurement impossible. Full details of the operation of the instrument can be found elsewhere [14, 15] but the basic principles are as follows. A roughly monochromatic beam is polarized with the neutron spin parallel to the beam direction. This now passes along the incident path in a fixed vertical magnetic field H_z , which causes the neutron spin to precess with the appropriate Larmour frequency. At the sample, the spin direction is reversed and the scattered neutron passes through an equal path length in the same field H_z , so that the precession direction is reversed and the precession 'unwinds' itself by the time the neutron reaches the spin analyser and the detector. The essential point here is that, although all the different neutron energies in the incident beam will precess to a different extent, after an elastic scatter they will all exactly unwind. Now, very small changes in either of the magnetic fields will cause the detected intensity to vary as a cosine function; thus if the minimum intensity is zero, the polarization is complete, i.e. the polarization $P_0(Q, t)$ for elastic scattering is defined by the equation

$$P_0(Q, t) = [I_{\max}(Q, t) - I_{\min}(Q, t)]/[I_{\max}(Q, t) + I_{\min}(Q, t)] \quad (1)$$

where, t is called the Fourier time and is given by $\pi N/E_0$ where N is the number of turns and E_0 is the mean incident energy. Thus, if both magnetic fields (precession rates) are increased together in steps and the polarization is remeasured at each value, the polarization will only decrease slowly, due to field inhomogeneities, etc. If we now introduce a quasi-elastic scatterer, the velocities after scattering will be spread out relative to the incoming value and the unwinding process will no longer be precise so that the polarization written $P_m(Q, t)$ will be reduced. Clearly, the higher the precession rate, the greater the loss of polarization. The properties of the quasi-elastic scatterer are therefore given by

$$P(Q, t) = P_m(Q, t)/P_0(Q, t). \quad (2)$$

It turns out that $P(Q, t)$ is proportional to $S(Q, t)$, the Fourier transform of the usual scattering function $S(Q, \omega)$; for many purposes the former is actually a more useful function for comparison with models.

Small-angle scattering data were obtained in two ways: first from the total count-rate in the detector with the analyser switched off and second by adding the spin-up and spin-down

count-rates. The measurements were made at angles between 1 and 16° and an incident wavelength of 6 Å was used. This gives Q values from 0.01 to 0.36 Å⁻¹. The spin-up and spin-down components are respectively given by

$$I_+(Q) = I_{\text{coh}}(Q) + I_{\text{inc}}^{\text{isotope}}(Q) + \left(\frac{1}{3}\right)I_{\text{inc}}^{\text{spin}}(Q) \quad (3)$$

$$I_-(Q) = \left(\frac{2}{3}\right)I_{\text{inc}}^{\text{spin}}(Q) \quad (4)$$

where the $I(Q)$ terms are the measured intensities, and details of the scattering cross-section terms in equations (3) and (4) are given in table 1.

Table 1. The spin- and isotope-incoherent scattering cross-sections.

| | % | $\sigma_{\text{inc}}^{\text{spin}} (10^{-28} \text{ cm}^2)$ | $\sigma_{\text{inc}}^{\text{isotope}} (10^{-28} \text{ cm}^2)$ |
|------------------|--------------|---|--|
| H ₂ O | $C_1 = 22.6$ | $(2\sigma_{\text{H}})_{\text{inc}}^{\text{spin}} = 159.6$ | $4\pi \sum_n C_n C_1 b_n (b_n - b_1) = 7.289$ |
| D ₂ O | $C_2 = 48.6$ | $(2\sigma_{\text{D}})_{\text{inc}}^{\text{spin}} = 4.00$ | $4\pi \sum_n C_n C_2 b_n (b_n - b_2) = 3.648$ |
| HDO | $C_3 = 28.8$ | $(\sigma_{\text{H}} + \sigma_{\text{D}})_{\text{inc}}^{\text{spin}} = 81.6$ | $4\pi \sum_n C_n C_3 b_n (b_n - b_3) = 6.920$ |

Because $I_{\text{coh}}(Q)$ includes the small-angle scattering, which would swamp the incoherent scattering in the relevant Q range, it is necessary to approximately match coherent scattering densities by use of the D₂O/H₂O ratio, which can be matched to the Vycor matrix. Figure 1 shows the typical small-angle scattering intensity versus Q measured on the LOQ diffractometer at the Rutherford Appleton Laboratory for the porous Vycor glass saturated with several D₂O/H₂O mixtures [16]. The sample saturated with 64% D₂O shows a nearly perfect match, i.e. the scattering intensity, $I(Q)$ is almost flat through the position of the peak at 0.025 Å⁻¹, due to the spinodal decomposition process that takes place in Vycor as part of the manufacturing process. Comparison with the 8% D₂O data (the ratio of isotopes that gives zero scattering density for water) shows that the peak is reduced by three orders of magnitude. When the 64% D₂O water mixture is used, the coherent scattering contribution $I_{\text{coh}}(Q)$ can be ignored. Hence the measurement of tracer diffusion coefficient can be simplified.

Because the quasi-elastic coherent scattering decay is the faster process present, we believe that our measured t range should be dominated by $I_{\text{inc}}(Q, t)$ and hence that the tracer coefficient D_t can be evaluated by a single experiment since

$$I_{\text{inc}}(Q, t) \propto \exp(-Q^2 D_t t). \quad (5)$$

2. Experimental results

The well characterized system, porous Vycor (7930), here used in its powdered form, is marketed by Corning. It consists of a borosilicate glass that has been allowed to undergo partial spinodal decomposition into its components. The B₂O₃ component is then removed by chemical etching, leaving about 28% by volume of interconnected pore space with a mean pore size of about 30 Å and an internal surface area of about 250 m² g⁻¹. A mixture of 64% D₂O/36% H₂O was prepared. The samples were dried by heating in a vacuum and then the three samples were equilibrated at 95% relative humidity in order to avoid water condensation on the surface of the container.

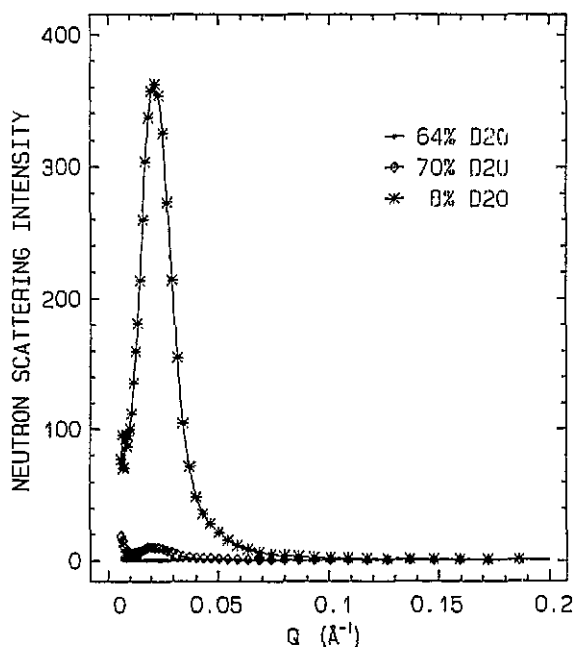


Figure 1. Comparison of small-angle neutron scattering from porous Vycor glass saturated with water mixtures as indicated in the figure. The sample saturated with 64% D₂O shows the best match with the Vycor matrix. The data for the 70% D₂O sample are also given to demonstrate the sensitivity of the peak intensity to the isotopic ratio.

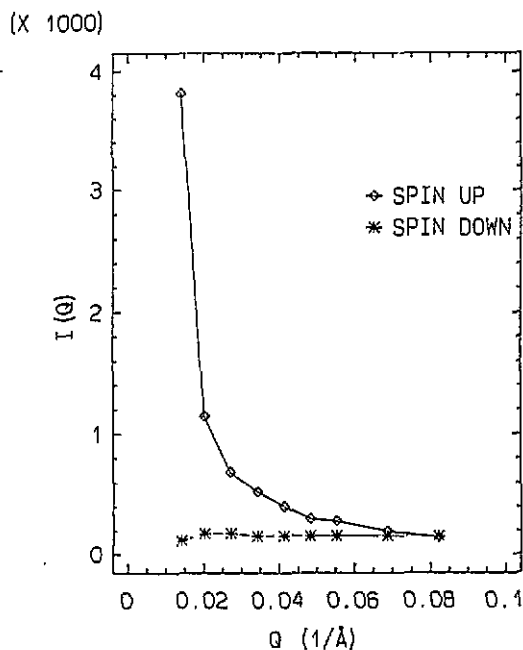


Figure 2. The total spin-up and spin-down intensities as a function of Q for porous Vycor glass saturated with 64% D₂O/H₂O mixture at room temperature.

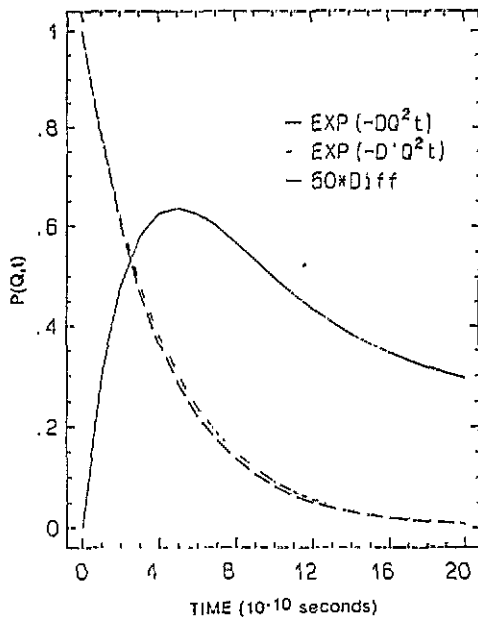


Figure 3. Plot of the two components of the exponential decays (dotted curves) and enlarged difference ($50\times$), i.e. $50P(Q,t)$ (smoothed curve) versus time.

Figure 2 shows the spin-up and spin-down intensities $I_+(Q)$ and $I_-(Q)$ respectively, for no precession field, as a function of Q for the Vycor saturated with the matched water

mixture at room temperature. The first measurement of the echo was made for this sample at $Q = 0.014 \text{ \AA}^{-1}$ (2° and 6 \AA). After measuring for 12 h, the echo was found to be very weak with no sign of an exponential decay as expected for this type of experiment [14]. As a result of several more trial runs, we finally found a very weak echo at higher Q . The resulting data are shown in figure 3. Although the statistics are not very good, the data clearly show a hump instead of the exponential decay. This hump shifts towards small t (or current) with increasing Q (i.e. $D_t Q^2 t_m = \text{constant}$ where t_m is t at the hump position). The first puzzle in these results is that the echo is so small at finite time, because we would have expected the coherent component to have decayed to zero and because, for our isotopic ratio, the spin-down cross-section exceeds the spin-up cross-section by more than 7 barns. The fact that the spin-down value slightly exceeds the spin-up one and yet the echo at small times increases and then decreases, giving the hump in the echo amplitude, suggests that there is more than one time decay with amplitudes of opposite sign and slightly different decay times, and that the spin-up scattering has a comparable amplitude but smaller D_t . One possible explanation for this unexpected result is that the different time constants originate from differences in the tracer diffusion coefficients of H_2O , HDO and D_2O which can be taken to be $D_t' = (\frac{18}{20})^{1/2} D_t$ for D_2O and $D_t'' = (\frac{18}{16})^{1/2} D_t$ for HDO , relative to the value of H_2O . A full analysis of this model would involve introducing isotope incoherent terms (see the appendix) which would not normally be considered in quasi-elastic scattering. As one knows, the total incoherent cross-section consists of two components [18], i.e.

$$\sigma_i = \sigma_i(\text{spin}) + \sigma_i(\text{isotope}) \tag{6}$$

where

$$\sigma_i(\text{spin}) = \sum_n \sigma_{i,n} = 4\pi \sum_n C_n (b_n^i)^2 \tag{7}$$

and

$$\begin{aligned} \sigma_i(\text{isotope}) &= 4\pi \sum_n \sum_{m>n} C_n C_m (b_n - b_m)^2 \\ &= 4\pi \sum_n \sum_{m>n} C_n C_m [b_n(b_n - b_m) + b_m(b_m - b_n)] \\ &= 4\pi \sum_n \sum_m C_n C_m b_n (b_n - b_m) \end{aligned} \tag{8}$$

where b_n^i and b_n are incoherent and coherent scattering lengths of the n th isotope, respectively, and c_n is its concentration. Differences of the coherent scattering cross sections among the three isotopes involved give rise to the isotope incoherent scattering, which has diffusion coefficients quite different from those of coherent quasi-elastic scattering (related to chemical diffusion) and is separated in a different time scale. We, therefore, could concentrate on the self-diffusion terms only. On the other hand, although the isotope contribution has similar behaviour to the spin incoherent contribution, because there are no neutron-nuclear spin interactions involved in the scattering, there is no phase change in the process of scattering: hence the isotope contribution is positive and proportional to the contrast between the moving $r_m(t)$ and static $r_n(0)$ isotopes, i.e. the $b_n(b_n - b_m)$ term. Therefore, the dynamical equation (5) has to be spelt out in detail (see the appendix). For the mixture of H_2O , D_2O and HDO with diffusion coefficients D_t , D_t' and D_t'' respectively, each contribution can be calculated according to its concentration (detailed cross-sections

for them are listed in table 1). Therefore, the dynamic structure factor contributed from the m th isotope is

$$S_m(Q, t) \propto \sum_n C_n C_m b_n (b_n - b_m) \exp\{iQ[r_n(0) - r_m(t)]\} \\ \propto \sum_n C_n C_m b_n (b_n - b_m) \exp(-D_t^m Q^2 t). \quad (9)$$

Hence, we have three different isotopic contributions (including the spin incoherent one): for H₂O

$$P(Q, t) \propto \left(4\pi \sum_n C_n C_1 b_n (b_n - b_1) - (C_1 \frac{2}{3} \sigma_H^{\text{spin}})\right) \exp(-D_t Q^2 t) = -4.68 \exp(-D_t Q^2 t) \quad (10)$$

for D₂O

$$P(Q, t) \propto \left(4\pi \sum_n C_n C_2 b_n (b_n - b_2) - (C_2 \frac{2}{3} \sigma_D^{\text{spin}})\right) \exp(-D_t' Q^2 t) = 4.10 \exp(-D_t' Q^2 t) \quad (11)$$

and for HDO

$$P(Q, t) \propto \left(4\pi \sum_n C_n C_3 b_n (b_n - b_3) - \frac{1}{3} C_3 (\sigma_D + \sigma_H)^{\text{spin}}\right) \exp(-D_t'' Q^2 t) \\ = -0.86 \exp(-D_t'' Q^2 t) \quad (12)$$

where b_1 , b_2 and b_3 represent the total coherent scattering lengths of H₂O, D₂O and HDO molecules, respectively. The C are the corresponding concentrations, which are produced by random walk processes in the large ice I_h structure containing ($50 \times 50 \times 50$ unit cells) 50 000 water molecules with 63% of D₂O.

As we can see, firstly, the contribution from HDO is very small compared with the other two terms and negative, as for H₂O; secondly, contributions from H₂O and D₂O are similar in magnitude, thus this could explain the weak echo signals in the experiment. The total echo amplitude has the form

$$P(Q, t) = -A \exp(-D_t Q^2 t) + B \exp(-D_t' Q^2 t) + C. \quad (13)$$

Figure 3 shows a model calculation for $P(Q, t)$, which does indeed show a broadened hump much like the experimental curve in figure 4, and the position of this hump does decrease with increasing Q as observed. Using this model the experimental data were fitted very well with three parameters, A , B and D_t (where $D_t' = (\frac{18}{20})^{1/2} D_t$) as shown in the smoothed curve in figure 4, giving values of D_t of $1.9 \pm 0.2 \mu\text{eV}$ for $Q = 0.07 \text{ \AA}^{-1}$, $2.8 \pm 0.3 \mu\text{eV}$ for $Q = 0.09 \text{ \AA}^{-1}$ and $4.2 \pm 0.3 \mu\text{eV}$ for $Q = 0.14 \text{ \AA}^{-1}$, which is about half of the value for bulk water at room temperature. We may compare the results with our previous measurement for water in porous Vycor using a 43% H₂O/D₂O water mixture, which is far from the matching condition [17]. These show a complicated exponential decay, implying that they result from a mixture of tracer diffusion and chemical diffusion, which cannot be separated one from another. However, in the present case using the matched water mixture, the chemical diffusion can be removed. However, a new problem is shown clearly in that the near cancellation of the echo at the contrast matching point and unexpected double relaxation process and the low count rates obtained on IN11 made the evaluation of the tracer diffusion coefficient difficult. The problem will be overcome when IN15—a similar instrument with multi-angle detectors—becomes available.

(X 1E-3)

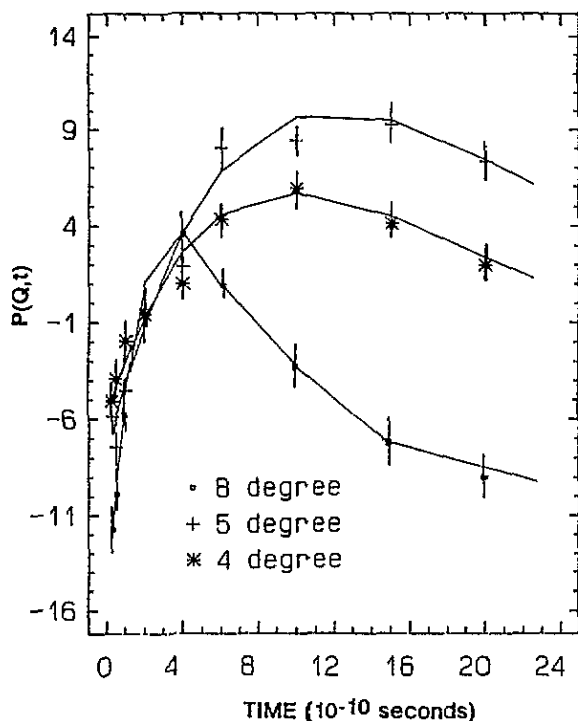


Figure 4. Plot of $P(Q, t)$ (with error bars) versus time at different Q values at room temperature. The smoothed curves are fitted with the model.

Appendix

According to neutron scattering theory, the elastic coherent scattering cross-section from a crystal within a unit of solid angle can be expressed as [18]

$$\frac{\delta\sigma_{coh}}{\delta\Omega} = \sum_i^N \sum_j^N b_i^* b_j \exp[i\mathbf{Q} \cdot (\mathbf{r}_i - \mathbf{r}_j)] \tag{A1}$$

where N is the total number of atoms in the system, \mathbf{Q} is defined by $\mathbf{Q} = \mathbf{k}_0 - \mathbf{k}_1$, where \mathbf{k}_0 and \mathbf{k}_1 are the incident and scattered wave vectors of the radiation, respectively, and the amplitude of $Q = 4\pi \sin \theta / \lambda$, where λ is the neutron wavelength and θ is the half scattering angle. The position vector \mathbf{r}_j is the j th nucleus in the sample and b_j is the coherent scattering length of the j th atom. If the nuclear spin and isotopes are uncorrelated, then

$$\sum_i \sum_j b_i^* b_j^* = \sum_i \sum_{j \neq i} b_i^* b_j + \sum_i |b_i|^2 = \sum_i \sum_{j \neq i} b_i^* b_j + \sum_i (|b_i^2| - |b_i|^2). \tag{A2}$$

The second term is the Laue scattering term, giving a flat background which we are not interested in. The scattering function can be regarded as containing three terms: static, dynamic and inelastic structure factors:

$$\frac{\delta\sigma_{coh}}{\delta\Omega} = \sum_i \sum_{j \neq i} b_i^* b_j [S_{ij}(\mathbf{Q}) + S_{ij}(\mathbf{Q}, t) + S_{ij}(\mathbf{Q}, E)]. \tag{A3}$$

In this paper, we are only interested in the dynamic term $S_{ij}(Q, t)$ relating to the diffusion properties of the system, therefore, the scattering cross section is

$$\begin{aligned} \frac{\delta\sigma_{\text{diff}}}{\delta\Omega} &= \sum_i \sum_{j \neq i} b_i^* b_j [S_{ij}(Q, t)] \\ &= \sum_i \sum_{j \neq i} b_i^* b_j \exp\{Q \cdot [r_i(0) - r_j(t)]\}. \end{aligned} \quad (\text{A4})$$

If b_i and b_j have different scattering lengths, the scattering mixes chemical and self-diffusion. To separate these we write $b_j = b_i + (b_j - b_i)$. Hence, we have

$$\sum_i \sum_j b_i b_j^* = \sum_i \sum_{j \neq i} [b_i^* (b_j - b_i) + |b_i|^2] \quad (\text{A5})$$

i.e.

$$\begin{aligned} \frac{\delta\sigma_{\text{diff}}}{\delta\Omega} &= \sum_i \sum_{j \neq i} [|b_i|^2 \exp\{Q \cdot [r_i(0) - r_j(t)]\} \\ &\quad + b_i^* (b_j - b_i) \exp\{Q \cdot [r_i(0) - r_j(t)]\}]. \end{aligned} \quad (\text{A6})$$

Therefore, the first term is a coherent chemical diffusion term and the second term is the self-diffusion function, because the scattering arises from the difference of the two different isotopes.

References

- [1] Schaefer D W and Keefer K D 1984 *Phys. Rev. Lett.* **53** 1383
- [2] Li J-C, Ross D K, Hall P L and Heenan R K 1989 *Physica B* **156 & 157** 185
- [3] Benham M J, Cook J C, Li J-C, Ross D K, Hall P L, Ross D K and Sarkissian B 1989 *Phys. Rev. B* **39** 633
- [4] Bishop M T, Langley K H and Karasz F E 1986 *Phys. Rev. Lett.* **57** 1741
- [5] Levitz P and Drake J M 1987 *Phys. Rev. Lett.* **58** 686
- [6] Beamish J R, Hikata A and Elbaum C 1983 *Phys. Rev. B* **27** 5848
- [7] Warnock J, Awschalom D D and Shafer M W 1986 *Phys. Rev. Lett.* **57** 1753
- [8] Even U, Rademan R, Jortner J, Manor N and Reisfeld R 1987 *Phys. Rev. Lett.* **59** 284
- [9] Dozier W D, Drake J M and Klafter J 1986 *Phys. Rev. Lett.* **56** 197
- [10] Alexander S and Orbach R 1982 *J. Physique Lett.* **43** L625
- [11] Rammal R and Toulouse G 1983 *J. Physique Lett.* **44** L13
- [12] Hall P L, Mildner D F R and Borst R L 1983 *Appl. Phys. Lett.* **43** 252
- [13] Katz A J and Thompson A H 1986 *Phys. Rev. Lett.* **54** 197
- [14] Mezei F 1972 *Z. Phys.* **255** 146
- [15] Mezei F et al 1980 *Neutron Spin Echo (Springer Lecture Notes in Physics)* ed F Mezei (Berlin: Springer) p 128
- [16] Li J-C, Ross D K and Benham M J 1991 *J. Appl. Crystallogr.* **24** 794
- [17] Tuck J J, Ross D K, Li J-C and Sarkissian B 1989 *Hydrogen Bonded Liquids, NATO Conf. Proc.* ed J C Dore and J Teixeira p 159
- [18] Price D L and Skold K 1986 *Methods of Experimental Physics* vol 23a, ed K Skold and D L Price (New York: Academic) p 1